MODELLING OF SCULL DRAG AT THE ORTHOGONAL POINT OF A ROWING STROKE

D. Hartwanger* E.A. Bunt†

(Received February 1996; Final version October 1996)

Model experiments (at half scale) were performed to determine the drag coefficient of two standard designs of scull, namely, the Macon and the Cleaver, at the position of the stroke when the oar is perpendicular to the boat. The measurement procedure involved the use of a gravity dynamometer to rotate a model blade through a limited angle in stationary water. It was found that the Cleaver blade showed on average a 3% improvement in blade efficiency – equivalent to only a 1.2% improvement in boat speed. The drag coefficient curve of the sculls as a function of the Froude Number Fr was similar to that experienced by a ship in shallow water in the region of the critical speed ($Fr_h = 1$); however, the drag coefficient peaked at a lower value of Fr than corresponds to the normal operating range of the blades ($1.4 < Fr < 2.2$). This suggests that an increase in blade drag – and hence in blade effectiveness – is possible if the operating Fr can be reduced so that normal oar operation occurs closer to the peak of the drag curve (where the drag coefficient was found to exceed by a factor of up to nearly 3 its value at higher values of Fr).

Nomenclature

List of symbols

a	inboard length of oar (m)
A	blade area (m^2)
b	distance from tholepin to centre of pressure (m)
b_L	blade length (m)
c	velocity of submerged cylinder (Fig. 3) (m/s)
C	hull resistance coefficient $(Ns^2/m^2)^1$
C_D	drag coefficient $\left(= D_o/\frac{1}{2}\rho V'^2 A\right)$
cp	centre of pressure ratio (= (distance from centre of pressure to blade tip)/(blade length)
d	average driving force (N)
D_o	maximum driving force (N)
F	reaction force at small radius from axis of rotation (N)
Fr	Froude number
F_o	maximum force applied to oar handle (N)
g	acceleration of gravity (m/s^2)
h	depth of test basin (m)
h'	depth of cylinder below surface (Fig. 3) (m)
G	movement of hull relative to combined centre of mass (m)
l	sculler's reach (m)
L_l	outboard length of oar (m)
M	applied moment (Nm)
pr	pivot ratio $(= (L_l - b + x)/b_L)$
P	power (W)
R	stroke rate (Hz)
R_o	resistance of hull (N)
Re	Reynolds number
t	time for which blade is in water (s)
T	total time for one stroke (s)
u	average hull velocity (m/s)
V	average speed of hull while blades are in water (m/s)
V'	oar velocity at centre of pressure (m/s)
x	distance of centre of pressure from axis of rotation (m)

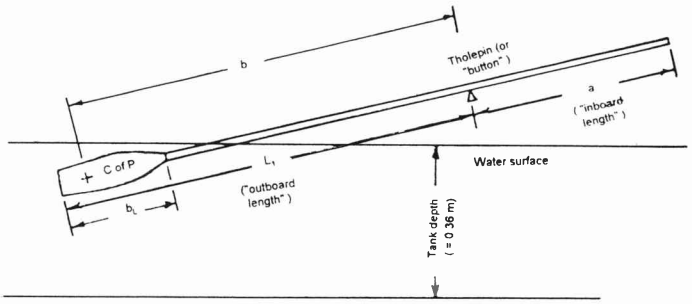

Figure 1 Definition sketch of oar and blade (Macon design)

Subscripts

c of p	centre of pressure
h	depth of test basin
m	model
p	prototype

*Graduate, School of Mechanical Engineering, University of the Witwatersrand, Johannesburg, P.O. Wits, 2050 South Africa
†Professor Emeritus, Honorary Fellow, SAIMechE

Greek

η	propulsive efficiency
θ_1	angle of oar at 'catch' with respect to the normal (rad)
θ_2	angle of oar at 'finish' with respect to the normal (rad)
λ	wave length (m)
ρ	density (kg/m^3)
μ	dynamic viscosity (kg/ms)
Ω	rate of rotation at normal oar position (rad/s)

Note on the definition of the Froude number Fr

Although Fr is generally defined in tenns of a velocity and a characteristic length dimension, in this paper different definitions are needed, depending on the particular wave phenomenon involved. For example, the well-known shallow water drag rise of ships (including rowing hulls) occurs at a unit value of $Fr = u\sqrt{gh}$, where u is mean hull velocity and h is water depth. In the theory referred to in Figure 3,[3] maximum drag occurs at $Fr = c/\sqrt{gh'} = 1$, where h' is the cylinder depth, while in the experiments referred to here, Fr is based on the tangential velocity V' of the oar in the water (at the centre of pressure of the blade) and on the depth of the centre of pressure of the oar blade below the free surface.

1 Introduction

Rowing is a sport which is now highly competitive; as a reshlt, in-house analyses of the drag characteristics of different oars are unlikely to be published by oar manufacturers to avoid premature exposure of possible design developments. The best scientifically oriented text on the subject of rowing is felt to be Scott and Williams,[1] published in 1967, which considers hydrodynamic, mechanical, biomechanical, physiological and psychological aspects of the sport – but which emphasises the insufficiency of the existing drag data and the difficulties attending the definition of an oarsman's capabilities. In a later work by Burnell,[2] published in 1989, the difficulty of quantifying the interaction of design and handler is also emphasised.

The actual motion of an oar is complex – and is therefore difficult to simulate. During the immersed portion of the stroke, an oar is subjected to a 'twisting' motion (as seen in plan view) as the boat, and therefore the point of attachment of the oar, moves forwards, resulting in a variation of drag force (see Figure 2, which was determined by strain gauge measurements on an actual full size oar). The peak of the drag curve shown occurs when the oar is approximately perpendicular to the boat. (The choice of the perpendicular position is arbitrary, since the location of the peak of the force curve naturally depends on the oarsman; however, it is approximately correct for all cases). Clearly the higher the drag forces experienced, the better the blade in the water will act as a fixed fulcrum about which the boat can be propelled by the lever action exerted by the oarsman, and so be more efficient. It is therefore of interest to consider whether the drag force is a function of any other variable than position, as it is well known that the drag of ships under 'shallow water' conditions peaks at a unity value of the Froude depth number $Fr_\mathrm{h} = u/\sqrt{gh}$. Such a drag peak is also illustrated in the calculated function in Figure 3 which represents the resistance of a submerged cylinder – which may be indicative of scull behaviour.

To examine whether the rowing technique might be optimised in respect of controllable variables, a model experiment was conducted in water, using a square test basin for drag measurements, to examine the drag variation as a function of the Froude number Fr. The two designs investigated, as shown in Figure 4, were the Macon, an older design dating back to the Olympic Games in the 1950s,[4] and the Cleaver, first used by the US team at the 1992 Olympic Games, and widely assumed to represent a superior design. The present experiment falls short of complete simulation of a rowing stroke, but concentrates on the effect of other variables on the peak drag occurring in the perpendicular oar position. Further experimental work is clearly required to examine drag effects over a complete simulated stroke.

2 Blade action

Figure 1 shows a definition sketch of an oar in its operating position, and Figure 5 shows the complicated sequence of movements of a scull relative to the water during a rowing stroke which occupies 80° – 100° of arc. A stroke is characterised by the 4 phases of 'catch, 'drive', 'finish', and 'recovery'. 'Catch' is defined as the entry of the blade into the water in a squared position; this is followed by the important 'drive' phase (application of the driving force), and is followed by the 'finish' (extraction of the blade from the water). In the 'recovery' phase the blade is out of the water while it is being returned in a feathered position to the 'catch' and is not considered here. In terms of oar design the 'drive' phase clearly has the most influence, but the skill of the oarsman also has a large effect in minimising resistance forces when the blade is extracted from the water, and in allowing maximum force to be applied at the moment of the 'catch'. Analysis will therefore be mainly concerned with the consideration of oar performance during the drive phase.

The flow of fluid around the blade during the stroke gives rise to both lift and drag forces both of which are utilised by the oarsman to varying extents. The drag force occurs in the same direction as the fluid velocity and the lift force at right angles thereto. In the 'catch'

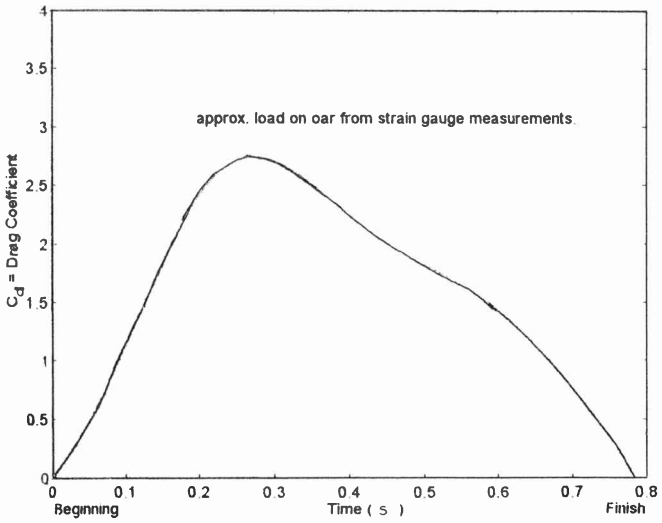

Figure 2 Strain gauge measurements on an oar during a stroke (from Scott & Williams).[1] Note: Boat speed stated to be not accurately known.

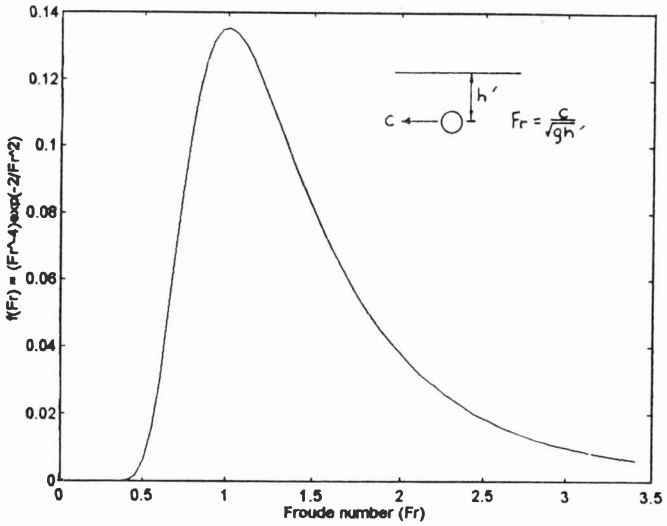

Figure 3 Theoretical resistance of a submerged cylinder (based on analysis in Yih).[3]

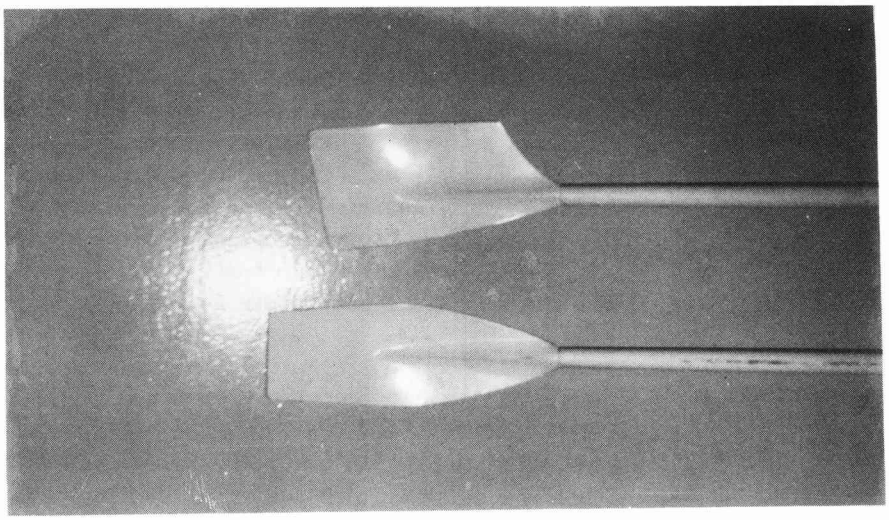

Figure 4 Photograph of model Macon (upper) and Cleaver (lower) blades.

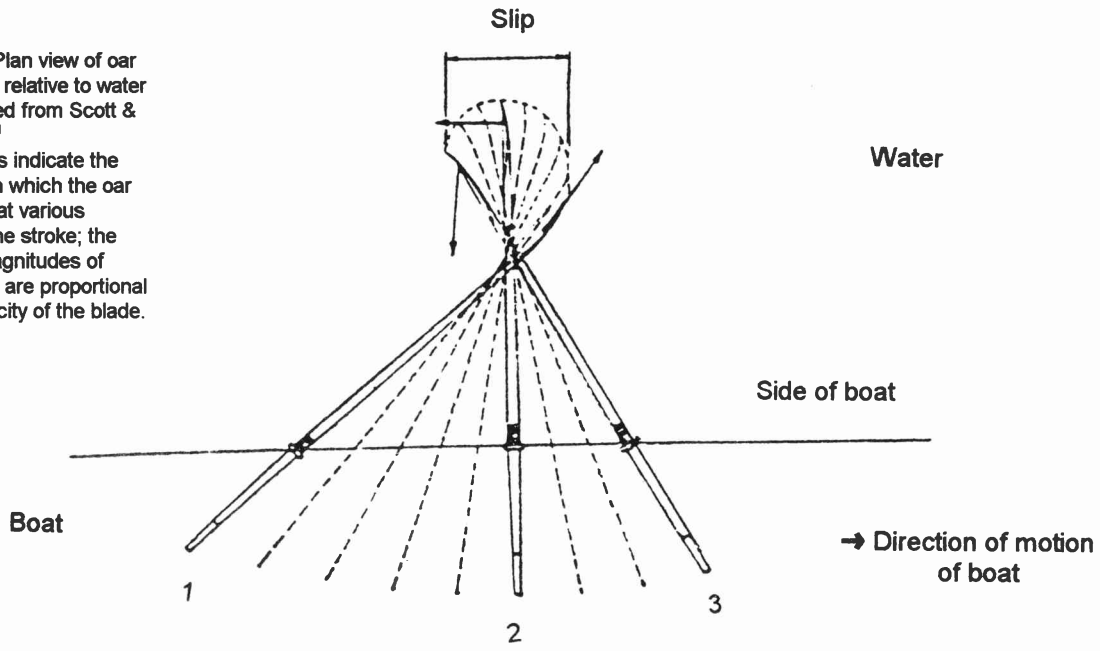

Figure 5 Plan view of oar movement relative to water (reproduced from Scott & Williams).[1]
The arrows indicate the direction in which the oar is moving at various points in the stroke; the relative magnitudes of the arrows are proportional to the velocity of the blade.

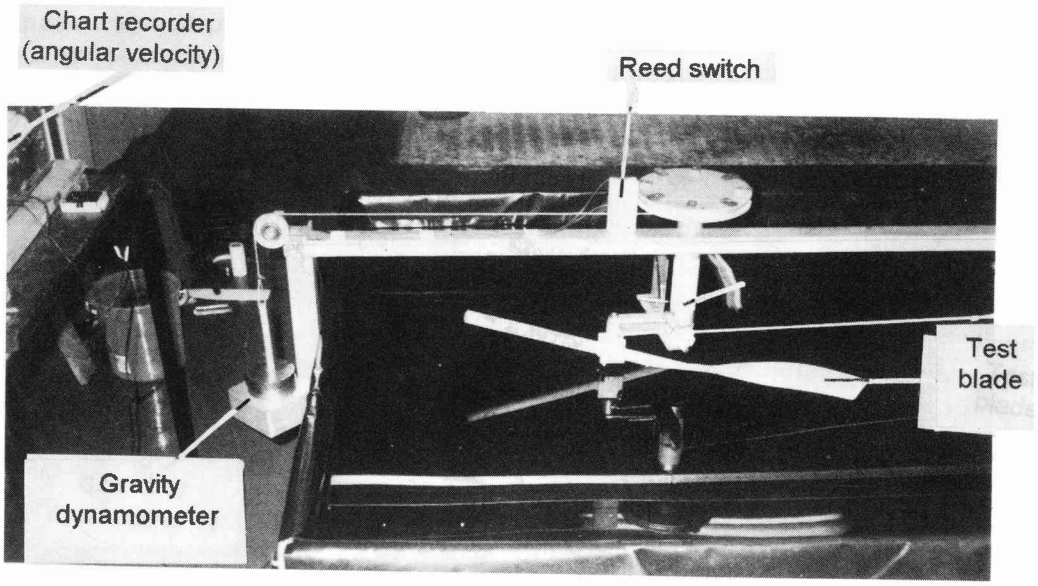

(a)

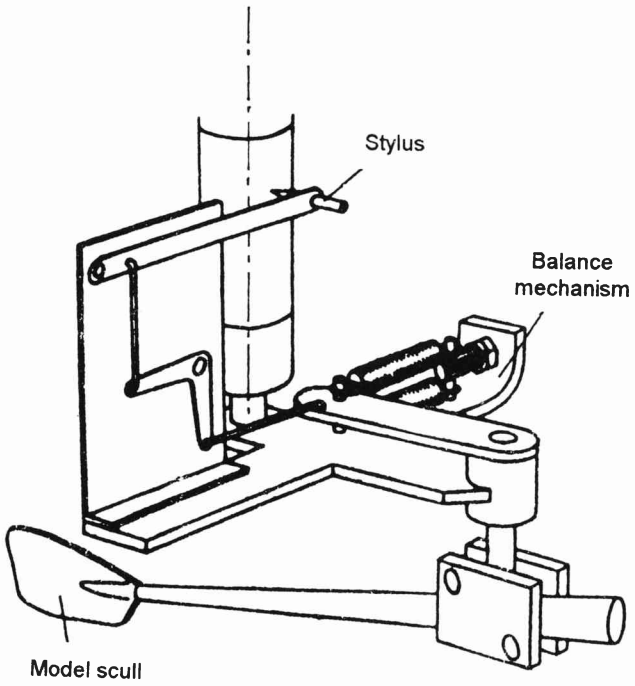

(b)

Figure 6 Details of towing tank
(a) Photograph of testing tank, with blade in stationary position
(b) Sketch of drag balance.

position (see Figure 5) the drag force is minimal, since the projected area of the blade normal to the fluid velocity is very small, while the lift force is substantially larger.

In the intermediate position, when the oar is perpendicular to the boat, the oar rotates in absolute terms about a point on its shaft, the instantaneous centre of zero velocity, relative to undisturbed water, which thus provides a means of relating the blade velocity to the boat velocity. This point has zero translational velocity relative to the undisturbed water, and is then the true pivot point of the oar (see Figure 5). In this position the lift force becomes zero and the drag a maximum. A large portion of the drag force, and hence boat acceleration, arises when the oar is in this perpendicular region. At the 'finish', there is a large decrease in the drag force induced by the oar. However, due to the movement of the oarsman on his slide relative to his boat at this moment, boat deceleration is avoided and peak boat velocity is actually achieved during the recovery phase.[5] It thus follows that in terms of oar design a primary goal is to increase the drag of an oar during the 'drive' phase – which also occurs when the body of the oarsman is in a particularly favourable position.

In a revelant analysis (Scott & Williams),[1] the point of rotation of the oar can be directly related to oar efficiency. The mechanics of oar propulsion can be simply presented[1] in terms of the following (basically 8) equations – which, however, depend on the validity of the following assumptions:

1. The driving force is at right angles to the shaft of the oar;
2. The drag force coefficient is constant throughout the stroke;
3. The speed of the boat hull is constant throughout the stroke;
4. The mean resistance of the hull is proportional to the square of the hull speed; and
5. The motion of the boat is 'straight and level' – but in practice the movement of the oarsman relative to the boat may cause pitching, which may have an effect upon the wave drag of the boat.

The propulsive efficiency is

$$\eta = V/b\Omega \tag{1}$$

The mean driving force is

$$d = (D_o/2\Omega t)\left(\theta_2 - \theta_1 + \frac{1}{2}\sin 2\theta_2 - \frac{1}{2}\sin 2\theta_1\right) \tag{2}$$

The time the blades are in the water is given by

$$t = (1/\Omega)\ln(\sec\theta_2 + \tan\theta_2/\sec\theta_1 + \tan\theta_1) \tag{3}$$

The maximum driving force is

$$D_o = \frac{1}{2}\rho C_D A V^2 (1-\eta)^2/\eta^2 \tag{4}$$

The mean speed of the hull during the time the blades are in the water is given by

$$V = u - G/t \tag{5}$$

The mean force on the oar is related to the resistance of the hull by

$$R_o = (t/T)\,d = Cu^2 \tag{6}$$

The power of the crew is given by

$$\eta P = R_o = Cu^3 \tag{7}$$

and the pull on the oar handle is related to the force on the blade by the equation

$$F_o = D_o b/a \tag{8}$$

In addition, a pivot ratio, pr, defined by

$$pr = (L_1 - b + x)/b_L \tag{9}$$

and a centre of pressure ratio, cp, defined by

$$cp = (L_1 - b)/b_L \tag{10}$$

have been introduced here to enable the response of the rowing system to be evaluated when various inputs are changed. V may then be expressed by

$$V = \Omega(L_1 - pr.b_L) \tag{11}$$

2.1 Dynamic similarity

In addition to geometrical similarity of blades and prototypes, equivalence of Froude numbers is required here for testing purposes since a scull operates at the water/air interface and hence is subject to wave action. In this case, where a model scale of 1/2 was used, equivalence was easily possible. Then in terms of the length characteristic L,

$$L_m = \frac{1}{2}L_p \tag{12}$$

Using equivalent Froude numbers, we have

$$Fr_p = Fr_m = V'_m/(gL_m)^{\frac{1}{2}} = V'_p/(gL_p)^{\frac{1}{2}} \tag{13}$$

which leads to

$$V'_m/V'_p = (L_m/L_p)^{\frac{1}{2}} = \left(\frac{1}{2}\right)^{\frac{1}{2}} = 0.707 \tag{14}$$

Since angular velocity (relative to the boat) of the model oar $\Omega_m = V'_m/(L_1)_m$ (where L_1 = outboard length of oar), we have

$$\Omega_m = (1/2)^{1/2} V'_p/\frac{1}{2}(L_1) = 1^{1/2}\Omega_p \qquad (15)$$

whence

$$\Omega_m/\Omega_p = 1.414$$

The model to prototype force ratio, assuming constancy of C_D, is given by

$$F_m/F_p = \frac{C_D\,(\text{area})_m\,\frac{1}{2}\rho V'^2_m}{C_D\,(\text{area})_p\,\frac{1}{2}\rho V'^2_p} = \frac{1}{4}\cdot\frac{1}{2} = \frac{1}{8} \qquad (16)$$

while the corresponding Reynolds number ratio is given by

$$Re_m = \frac{\rho L_m V'_m}{\mu} = \frac{\rho}{\mu}\left(\frac{1}{2}L_p\right)\left(\frac{1}{2}\right)^{\frac{1}{2}} V'_p = Re_p/2\sqrt{2}$$

so that

$$Re_m/Re_p = 0.354 \qquad (17)$$

Taking typical values of V'_m as 0.34 m/s, L_m as 4 × (hydraulic mean depth of blade) = 114.8 mm (Macon value), and a water temperature of 20°C, $Re_m = \frac{0.1148\times 0.34}{1.005\times 10^{-6}} =$ 38 840 and $Re_p = 38\,840/0.354 = 109\,700$ both of which values fall within the flat portion of a typical C_D *vs* Re curve for fully immersed bluff bodies of corresponding geometry such as flat plates, and equality of Re (which cannot simultaneously be satisfied) is therefore not expected to be critical, provided flows are turbulent. (This curve is flat to $Re = 15\,000$, corresponding to a value for V'_m as low as 0.13 m/s).[6]

3 Experimental Equipment

As indicated earlier, the point in the stroke when the drag force is a maximum, namely, the perpendicular position, was used as a basis for simulating oar movement for purposes of determining the drag coefficient for each design. This was achieved by rotating a scale model blade about its true pivot point in stationary water. All velocity vectors were then perpendicular to the blade. This procedure meant that drag readings were made under steady state conditions – as compared to a continuously varying flow pattern during an actual stroke; as the forces measured reached an equilibrium value very quickly after starting (in fact, within 0.3 s), the flow patterns achieved could be considered a good simulation of those occurring when the oar position corresponds to the perpendicular position on the prototype. Tests were performed at typical values of the inclination of the oar with respect to the water surface and of the depth of the blade below the surface, as described below under Experimental procedure.

3.1 Blades

The two blades shown in Figure 4 were geometrically similar models of actual blades and were manufactured to a high degree of accuracy of 3 mm beaten aluminium plate which had been glued to shaped wooden shafts. Body filler was used to perfect the rib profile. The projected area of each blade was calculated both by Simpson's Rule and by drawing the outline of the blade onto a card which was then cut out and weighed on a scale with a resolution of 10^{-4} N. The area of the shaft which was submerged was then calculated and added to that of the blade. Table 1 shows these details. As seen in Figure 4, the Macon design is symmetrical, whereas the unsymmetrical Cleaver design presents an almost horizontal lower edge to the water at entry, while in the 'drive' position it is the upper edge that is almost horizontal.

Table 1 Model blade areas

Type	Area, mm²	Shaft area, mm²	Total area, mm²
Macon	175 200	15 300	190 500
Cleaver	185 600	11 900	197 500

3.2 Testing Tank

The test tank is shown in Figure 6(a). It consisted of a water basin about 1.1 m × 1.1 m, with a water depth of 0.36 m, adapted for circular motion of the model blade through stationary water, and it incorporated a gravity dynamometer for drag measurement, as used in simple ship towing basins. The gravity dynamometer consisted of a weight attached to a string which passed over one pulley with its axis horizontal, and rotated another larger pulley to whose vertical spindle the model blade was attached; this spindle also supported a paper drum to record blade force. Release of the weight thus rotated the model blade steadily after an initial acceleration period of approximately 0.3 s.

The larger pulley was also used for angular velocity measurement of the model oar. After starting, the velocity of rotation of the model oar rapidly reached a constant velocity (as deduced from chart measurements) which it maintained for approximately 100°. The velocity of the model oar relative to the stationary water spanned an approximate velocity range of 0.3 to 0.6 m/s during the experimental program.

Recording devices were essentially mechanical in character. The actual drag measuring device shown in Figure 6(b) consisted of a series of levers to magnify the small deflection of the oar. This deflection was due to

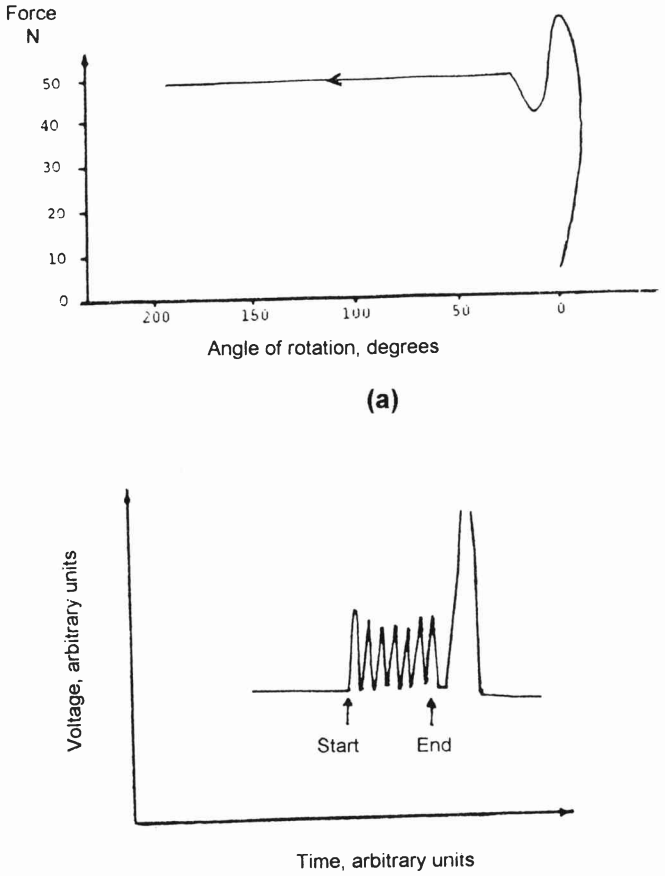

Figure 7 Chart records during stroke (Macon blade)
(a) Force
(b) Angular velocity

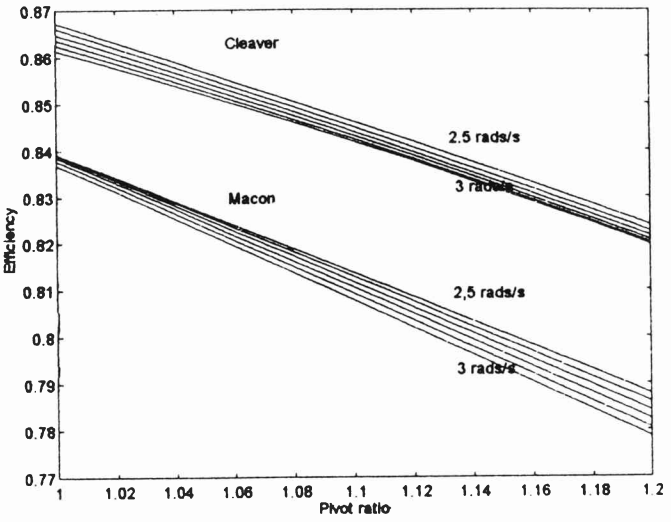

Figure 11 Blade efficiencies as a function of *pr* and Ω.
• (The curves are spaced at equal increments of Ω.)

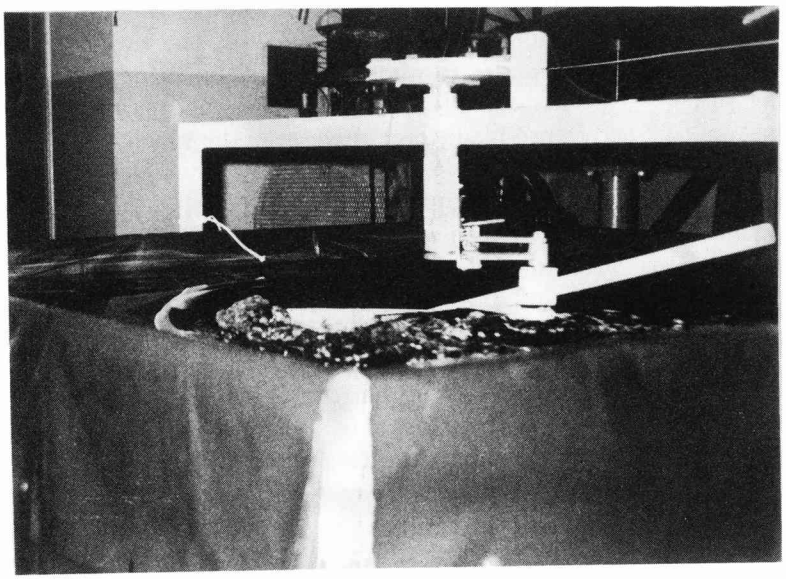

Figure 8 Photograph of model oar in motion

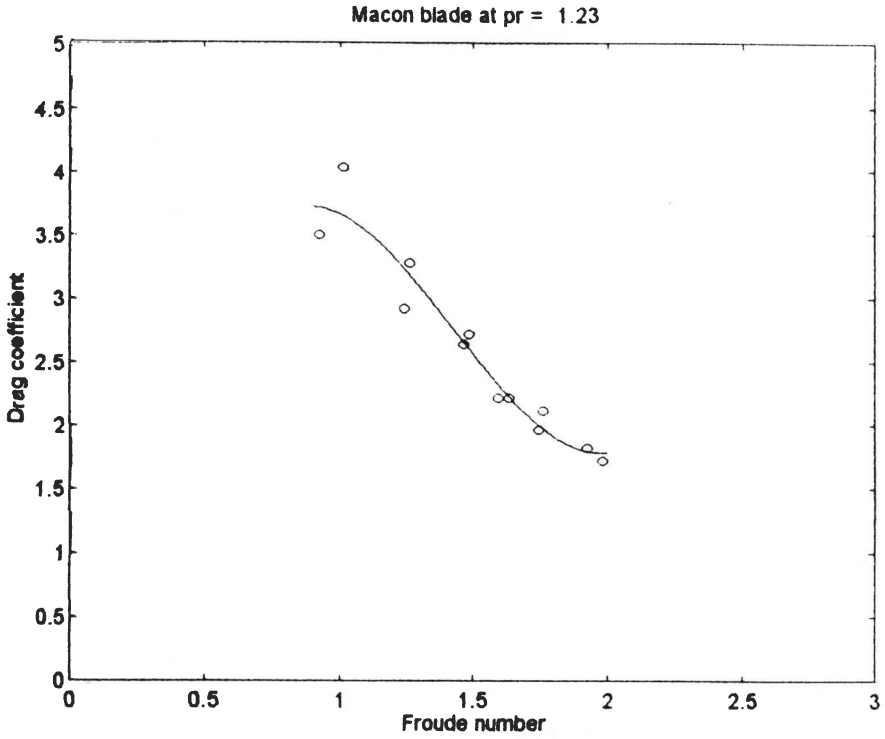

(a)

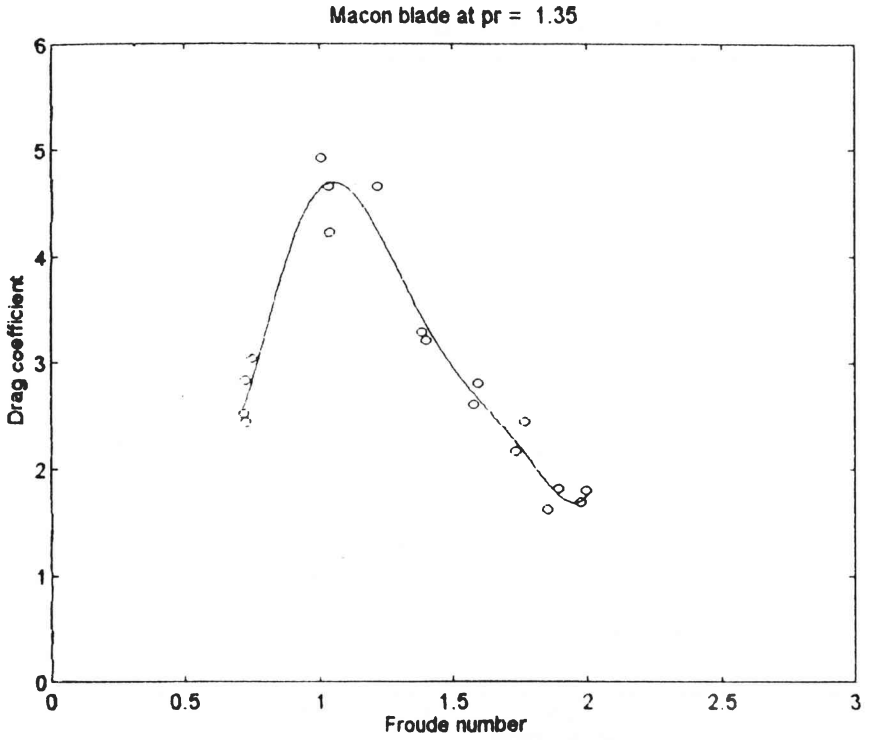

(b)

Figure 9 Drag coefficient *vs Fr* (Macon blade) as a function of *pr*
(a) At *pr* = 1.23
(b) At *pr* = 1.35

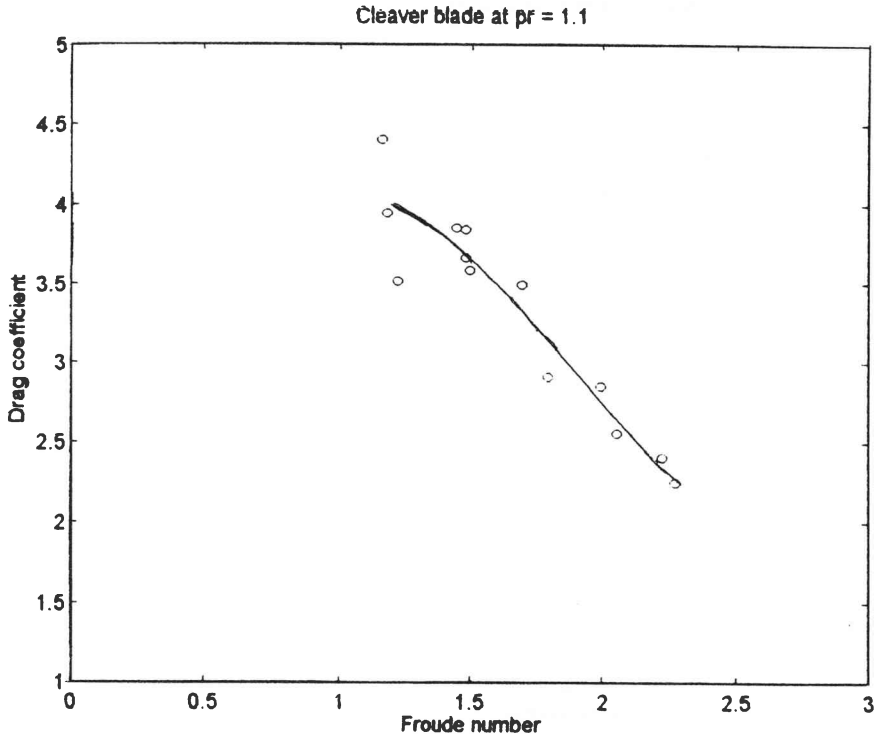

(a)

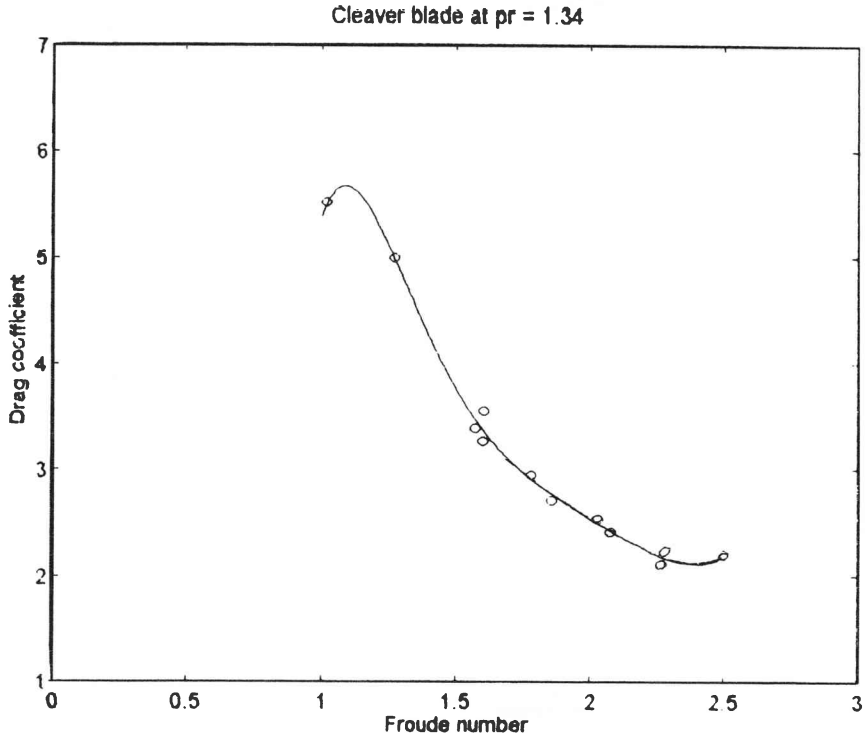

(b)

Figure 10 Drag coefficient *vs Fr* (Cleaver blade) as a function of *pr*
(a) At *pr* = 1.1
(b) At *pr* = 1.34

a moment set up about a point at an arbitrary radius from the primary axis of rotation, and which was resisted by the reaction force provided by two springs at the end of a small arm. The deflection of the small arm was then magnified in order to displace a stylus which recorded on a paper drum attached to the main spindle. The vertical deflection of the stylus was thus directly related to the force applied to the springs to record a graph of force *vs* angular displacement of the spindle (which rotated as the weight descended) and hence of the model oar. In addition the secondary axis allowed a second moment equation to be generated which was needed in order to solve for the two unknowns, ie. the drag force and its location. This recording device is similar in principle to the mechanical (pressure) engine indicator of the Crosby, Maihak or Dobbie-McInnes types (Sweeney)[7] and a typical 'indicator diagram' is shown in Figure 7(a). Calibration of this device is described below. Measurement of angular velocity was made by securing a series of magnets to the main pulley at precise 45° intervals. In close proximity to the pulley was placed a reed switch (which closed as each magnet passed it). The reed switch was connected between a low voltage supply and a chart recorder to indicate angular velocities as shown by the chart record of Figure 7(b). Figure 8 shows a photograph of the apparatus with the model oar in motion, showing the build up of water in front of the oar. An interval of 5 min between experiments was found to be sufficient for surface wave motions to die out.

3.3 Experimental procedure

Calibration of the experimental rig involved the use of a spring balance mounted on the end of a wooden shaft secured in the clamp used for holding the blades. (This spring balance was thus used to simulate the force acting on a blade when it was moved through the water.) This enabled two relationships to be determined – firstly, the actual moment experienced by the oar for a given applied moment, and secondly, the force exerted on the model oar by the spring for a given displacement on the recording graph. In both cases a linear relationship was obtained, as given by the following equations:

Actual moment = 0.9917 × (Applied moment) − 0.0162 Nm

Force exerted = 1.0672 × (Displacement on graph in mm) + 5.0482 N

From these results the values shown in Table 2 for sensitivity, accuracy, and repeatability were determined.

In this table, sensitivity was defined as

$$\text{Sensitivity} = \frac{\text{Rate of change of output}}{\text{Rate of change of input}}$$

Table 2 Calibration details

	Moment calibration	Force calibration
Sensitivity	0.991 7	1.067 2
Accuracy	± 0.58%	± 1.69%
Repeatability	0.12%	0.73%

Accuracy was defined as the maximum deviation as a percentage of full scale output, and repeatability as the maximum hysteresis as a percentage of full scale output.

In total, 140 tests were performed, comprising between 10 and 12 tests at each of 6 different pivot points for each of the 2 blades. These enabled the drag coefficient to be determined with respect to the point of rotation and at various rates of rotation. The following procedure was followed for each test:

1. The model oar was clamped in an upright (zero pitch) position at an angle of 15° to the horizontal. (In this position a point on the top end of the blade, at 100 mm from the blade origin, was maintained 10 mm below the still water surface).
2. The distance between the point of rotation and the blade tip along the axis of the 'loom' was recorded.
3. The system was placed in the starting position and masses (in steps of 480 g) placed on the gravity dynamometer support.
4. With chart recorder and chart stylus operating, the system was released to achieve a total oar displacement of 180°.

Figure 7(a) shows that the force measurement reached an 'orthogonal' (steady state) value almost immediately.

4 Results and discussion

As might be expected from their geometrical differences, the blades behaved somewhat differently in respect of both drag coefficient C_D and centre of pressure ratio *cp* as a ftmction of pivot ratio *pr*. Figures 9 and 10 show the drag coefficient of the two blade designs in terms of *Fr* (based on the depth of the blade at the centre of pressure) and *pr*, and Figure 11 the blade efficiencies (also in terms of *pr*) as calculated from Eq. 1. In the latter case the difference in propulsive efficiency (Eq. 1) of the Cleaver blade over the Macon blade is seen to amount to only about 3% – which corresponds to a speed difference of only 1.2%. It is of interest that a recent comparison of Olympic results (Nolte[8] shows that the extra boat speed achieved in using the Cleaver blade (as compared with

the Macon) was in one case only 0.2% and in another case, 0.4%.)

For purposes of calculation of Fr the length characteristic was arbitrarily taken as the depth below the surface, when the blade was stationary, of the top edge of the blade at the distance of the centre of pressure of the blade – since no meaning can here be attached to a dimension in the direction of motion, as is normally used in the analysis of ship data. This depth varied between 10 and 12 mm for the model Cleaver blade, and between 15 and 20 mm for the Macon blade, depending on oar inclination.

In 'shallow water' – the definition of which (Sabersky & Acosta)[9] may be interpreted in terms of λ/h, where λ, is the wavelength of the surface waves set up by the moving body – the drag of ships peaks at a value $Fr \approx 1$ (Lewis),[10] when the ship travels at the velocity of propagation of surface waves, the height of the drag peak increasing as the depth decreases. The extra drag is associated with wave making resistance. The effect of water depth on oar drag has not so far been pursued.

The similar shape of the curves shown in Figures 9 and 10 suggests that these experimental results are associated with 'shallow water' wave behaviour (for which $h/\lambda \ll 1$) but more work is required (observation of wave motion) to confirm this as well as an extension of data into the lower Fr range, particularly for lower values of pr (which are more likely to be encountered in practice) since a comparison of Figures 9 and 10 also shows that the curves are more complete at the lower end of the range for the higher values of pr, when the peak is also higher. The latter finding is perhaps to be expected, since this condition represents a greater effort on the part of the oarsman.

The greater efficiency, together with the higher peak values of C_D exhibited by the Cleaver blade, may be interpreted to indicate a superior flow pattern associated with this design. However, oarsmanship also enters into the comparison, as the larger area of the Cleaver blade (and especially its larger vertical dimension) makes it slightly more difficult to operate at the 'catch' and at the 'finish'. The Cleaver is of most benefit to an oarsman who is capable of mastering the blade in the water, whereas the Macon blade is a compromise design for use by a slightly less skilful oarsman or one with a less suitable style.

Further work needs to concentrate on the effect of depth, both that of the tank and that of the submergence of the oar, and of the effect of the angle θ_1 of entry of the oar into the water, in a more complete simulation of the whole stroke, for purposes of comparison with Figure 2.

An appendix offers an example of the use to which the various equations cited may be used to calculate operating conditions of interest.

5 Conclusion

1. At the water depth of the experiments performed (0.36 m), the peak value of scull drag (at the perpendicular oar position) is a strong function of Fr; the shape of the drag curve is similar to that found in the testing of other surface or sub-surface moving bodies. This is indicative of wave action effects.

2. C_D has a peak value during the stroke which exceeds by a factor of 2 or 3 that of a flat plate moved in a single fluid medium in a corresponding Re range, and corroborates strain gauge measurements of drag made during a full scale oar stroke. Away from the peak, C_D appears to level off at close to the flat plate value of C_D in a single medium. (As indicated in the Experimental procedure, every point of the graphs of C_D *vs* Fr represented a single test under steady state conditions).

3. The model Cleaver blade efficiency exceeded that of the Macon by 3%.

4. The model experiments suggest that rowing technique may be optimised by shifting operating parameters so that Fr is closer to the maximum drag position. (However, varying depth may have a bearing on both rowing technique and even choice of oar design). Additionally, since A is in the denominator of the expression for C_D, operation at peak C_D could lead to the use of a smaller, and therefore lighter, blade – which would help the endurance of the oarsman – although this effect is not likely to be a major one. Clearly, any reduction of mass in any component of the rowing system will be desirable.

References

1. Scott AC & Williams JGP (ed.). *A rowing scientific approach*, KM Ward, 1967.

2. Burnell R. *The complete sculler*, Sports Books Publisher, Toronto, 1989.

3. Yih C. *Fluid Mechanics*, McGraw-Hill, 1969.

4. Sayer B. *Rowing and sculling*, Robert Hale, London, 1989, p.106.

5. *Ibid*, p.54

6. White FM. *Fluid Mechanics*, 2nd edn, McGraw-Hill, NY, 1988.

7. Sweeney RJ. *Measurement Techniques in Mechanical Engineering*, Wiley, New York, 1953, p.118.

8. Nolte V. Do you need hatchets to chop your water? *American Rowing*, July/August 1993, p.23.

9. Sabersky RH & Acosta AJ. *Fluid flow*, Collier-Macrnillan, 1964.

10. Lewis EV (ed.). *Principles of Naval Architecture*, 2nd revised edn, SNAME, NY, 1988.

Appendix

The theory set down above may be used in a theoretical example of blade behaviour, and a calculation was made of the most suitable setting for the 'button' on the scull, assuming the following input values:

Table 3 Input values for rowing system

V	(average boat speed)	4.545 m/s
C	(hull resistance coefficient)	0.93 Ns^2/m^2
$a + L_i$	(overall oar length)	2.98 m
T/t	("stroke rhythm")	2.8
A	(blade area)	0.076 2 m^2
l	(sculler's reach)	1.25 m
G	(movement of hull relative to combined c.g.)	0.3 m
θ_2	(oar exit angle)	35°

The following outputs are required:

blade efficiency η
stroke rate R
force on oar handle F_o

These can be evaluated by graphical iterations; using a as the independent variable, the values shown in Table 4 can be calculated from Eqs. 2, 3, 5, 6, and 8:

Using Eq. 11 and assuming a value for pr, a corresponding value for Ω may be calculated. (V is obtained from Eq. 5, using an average value of t). C_D and η may be found by plotting pr and Ω on the blade curves, and Eq. 4 is then used to obtain d, which is compared with the value for D_o given above. If the estimate is too high, pr must be reduced until agreement is obtained. The results shown in Table 5 are then obtained.

It will be seen that the effect of changing variable a has a minimal effect on η, but a large effect on R and F_o. The analysis can be applied to evaluate the effect of changing such variables as $(a + b)$, A, ρ, blade type, and boat resistance. In addition to improving η, it is clear that an oarsman operating at reduced 'pull' needs to increase his stroke rate to maintain adequate power output – as is evident from the near-constancy of the product of the last two columns in Table 5.

Table 4 Output values (θ_1, Ωt, d/D, and D_o) for Macon blade

a(m)	θ_1 (deg)	Ωt (rad)	d/D	D_o (N)
0.88	57.9	1.899	0.6692	80.4
0.89	56.2	1.844	0.6844	78.6
0.90	54.6	1.795	0.6980	77.1
0.91	53.1	1.751	0.7104	75.7
0.92	51.7	1.711	0.7216	74.5

Table 5 Output values (η, b, T, R, and F_o) for Macon blade

pr	Ω (rad/s)	η (%)	b (m)	T (s)	R (Hz)	F_o (N)
1.08	2.700	81.7	1.909	1.969	30.5	174.4
1.07	2.710	82.0	1.895	1.905	31.5	167.4
1.06	2.720	82.3	1.882	1.848	32.5	161.2
1.05	2.730	82.5	1.870	1.796	33.4	155.6
1.04	2.735	82.7	1.862	1.752	34.3	150.8